Atomic-scale friction experiments reconsidered in the light of rapid contact dynamics

S. Yu. Krylov* and J. W. M. Frenken
Kamerlingh Onnes Laboratory, Leiden University, P.O. Box 9504, 2300 RA Leiden, The Netherlands
(Received 30 July 2009; revised manuscript received 25 November 2009; published 30 December 2009)

We present the first fully quantitative and self-consistent analysis of atomic-scale friction, explicitly taking into account the flexibility and low effective mass of the mechanical nanocontact. In a procedure, which is free of the traditional assumptions with respect to the corrugation of the interaction potential of the contact, the basic but experimentally inaccessible system parameter, we arrive at an excellent description of recent nanotribology experiments, including the transition from stick slip to nearly frictionless sliding. We show that, contrary to original interpretation, the ultralow friction observed in some experiments has been largely due to thermal (thermolubricity) rather than mechanistic effects (superlubricity). Furthermore, we observe the manifestations of two different forms of thermally induced sliding dynamics, namely, true thermolubricity (slipperiness based on thermal excitations) and a specific, low-dissipation type of stick-slip motion.

DOI: 10.1103/PhysRevB.80.235435 PACS number(s): 46.55.+d, 07.79.−v, 81.40.Pq

I. INTRODUCTION

With the application of atomic force microscopes to friction (friction force microscopy—FFM) (Ref. 1) atomic-scale access has been acquired to the origin of dissipative surface forces, boosting the rapidly developing field of nanotribology.[2] The FFM tip is believed to represent a single asperity, like the ones that constitute the contact between macroscopic sliding bodies. Typical FFM experiments demonstrate *stick-slip* (SS) motion of the tip over the substrate surface, reflecting mechanical instabilities that are considered to be at the origin of energy dissipation. A "milestone" in nanotribology has been the observation of the transition from SS to nearly frictionless sliding, induced by a reduction in the contact potential corrugation.[3,4] This seemed to confirm a general prediction of the traditional one-spring theories (see, e.g., Ref. 5) that if the corrugation falls below a critical value, depending on the driving spring stiffness, there are no mechanical instabilities and the system should exhibit continuous, nearly frictionless sliding, a regime called *superlubricity* (SL).

As has been recognized recently,[6–10] the traditional one-spring models strongly oversimplify the physics of friction. The flexibility of the tip apex calls for at least a *two*-spring model. This second spring introduces a wealth of new dynamics. The effective mass m, representing the inertia of the tip's bending motion, is associated with the flexibility of no more than 100 atomic layers at the apex.[7] The corresponding estimate for m is on the order of 10^{-20} kg, i.e., 9 to 12 orders of magnitude below the combined mass of cantilever+tip, M. Due to its ultralow effective mass, the tip apex can perform rapid activated jumps between the substrate potential wells while the measuring system (M) only sees the tip's mean position. As a consequence, thermal effects not only play an assisting role by activation of early slips, as in a one-spring model[11,12] but can also fully dominate the motion, leading to complete or partial delocalization of the contact on the long time scale of the motion of M.[8] Indirect indications for such behavior have been found in the comparison of the theory[8] with a high-resolution FFM experiment.[6] Thermal delocalization leads to several new scenarios of energy dissipation.[7,9,10] For example, the transition from SS to true, mechanistic SL can go through a regime of extreme, thermally induced reduction in friction, *true thermolubricity* (TL), or via a peculiar regime of low-dissipative stick slip (*stuck-in slipperiness*, SinS). These insights motivate a critical reinterpretation of FFM experiments.

In this paper, we report the first fully quantitative and completely self-consistent analysis of FFM experiments. Our results are threefold. First, we show that the traditional one-spring analysis can be fully misleading by a fatal underestimate of the true potential corrugation, the basic system parameter that is never known in advance. Second, we introduce a natural analysis procedure, based only on observables, the mean friction force, $\langle F \rangle$, and the maximal lateral force, $\langle F_{\max} \rangle$. The relation between these two quantities reflects the dissipation mechanisms at play and is found to be universal, i.e., points corresponding to different combinations of the unknown potential corrugation, effective mass of the contact and several other parameters collapse onto a single curve. This enables us to verify the consistency between theory and experiment avoiding any *a priori* assumptions about the unknown potential corrugation and the effective mass of the contact. Then, from a more detailed analysis, the contact corrugation can be found with a remarkably high precision, in spite of the remaining uncertainty in the exact value of m. Finally, the excellent match between theory and measurements (both in the $\langle F \rangle$-vs-$\langle F_{\max} \rangle$ plot and in detailed behavior of the lateral force as a function of time or support position) allows us to conclude that in the "superlubricity" experiments of Refs. 3 and 4, the friction force actually has become vanishingly low because of true TL and SinS, respectively, rather than mechanistic SL.

II. CALCULATION RESULTS

The results below have been obtained from calculations following a hybrid computational scheme described in Ref. 8. In short, the numerical solution of a Langevin-type equation for M is combined with Monte Carlo simulations for activated motion of m. The pre-exponential factor of the jump rate is approximated by the vibrational frequency at the

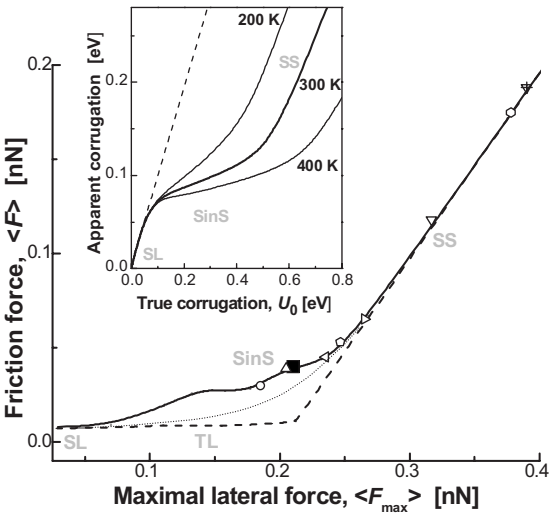

FIG. 1. Universal relation between basic observables, namely, the mean friction force and maximal lateral force. The solid curve was calculated by varying the potential corrugation U_0 for values of the other experimental parameters (specified in the caption of Fig. 3) typical for a soft driving system. Symbols correspond to $U_0=0.3$ eV and different combinations of the temperature and the effective mass of the tip apex, $T=300$ K and $m=10^{-20}$ kg (solid square), $m=10^{-23},10^{-17},10^{-14},10^{-12},10^{-11}$ kg (triangles), and $m=10^{-20}$ kg and $T=100,200,400$ K (hexagon, pentagon, circle). The dashed curve was calculated for the same k_{eff} but with $K=30$ N/m and $k=1.9$ N/m, i.e., for the case of a hard driving system. Different regimes of friction are indicated: ordinary SS, SinS, true TL, and SL. The dotted curve corresponds to the conventional one-spring model (Ref. 13) which does not distinguish between SinS and TL. The inset shows the relation between the apparent and the true potential corrugations. The dashed line in the inset corresponds to the mechanistic Prandtl-Tomlinson model, which implies $U_0^{(\mathrm{apparent})}=U_0$.

bottom of the well. The motion of M is assumed to be nearly critically damped while the level of thermal noise is related with the damping factor according to the fluctuation-dissipation theorem. The system is characterized by the cantilever (K) and tip (k) stiffness, temperature T, scanning velocity V, substrate lattice spacing a, and the amplitude of the contact corrugation U_0. A one-dimensional (1D) geometry and a sinusoidal tip-surface interaction potential (free energy) are assumed.

In real FFM experiments, the potential corrugation U_0 varies from scan line to scan line. Usually, one tries to extract it from the maximal lateral force recorded. According to the simplest, mechanistic Prandtl-Tomlinson model (see, e.g., in Ref. 5), $U_0^{(\mathrm{apparent})}=aF_{\mathrm{max}}/\pi$. How wrong this estimate is, is illustrated by the inset of Fig. 1, which shows the relation between the apparent and the true potential corrugations, calculated for a typical set of system parameters. At room temperature the difference can be as large as a factor 3.5; at elevated temperatures it is much stronger. The physics behind this result is straightforward. At high corrugations, in the SS regime, F_{max} is reduced with respect to its limiting value, $\pi U_0/a$, due to thermally activated jumps, which initiate slips to occur prior to the positions of mechanical instability. The result of this known effect[11,12] turns out to be very strong for the two-spring model in view of the high jump rate associated with the tip apex. At lower potential corrugations the rate of activated tip apex jumps becomes so high that the massive measuring system cannot follow them but sees only the mean position of the tip. The weak variation in $U_0^{(\mathrm{apparent})}$ seen in this range of U_0 is consistent with our earlier analytical calculation;[7] it reflects the fact that the corrugation of the effective tip-surface interaction, averaged over the rapid activated jumps of the tip's apex, only weakly depends on the true surface corrugation. The difference between apparent and true values disappears only at very low corrugations, when the apex always experiences a single energy optimum and the sliding motion is in the regime of SL.

Of course, differences between the apparent and true corrugations of the potential have been recognized also within the traditional one-spring model. However, within this model, it is difficult to imagine that these could be large; for that one would have to imply very high rates of thermally activated jumps, incompatible with the macroscopically large mass of the "jumping object." By contrast, the two-spring description, undoubtedly more realistic, reveals these rates to be extremely high as a natural consequence of the ultralow effective mass of the tip apex.

Underestimating energy barriers by a factor 3 or more is really dramatic since this leads to a fatal underestimate of the thermally activated rates by orders of magnitude. How should one (re)analyze FFM experiments when the decisive parameter, U_0, cannot be obtained directly? We propose an analysis that restricts itself completely to measured quantities, namely, the mean lateral force, $\langle F\rangle$, also referred to as the friction force, and the average maximum value, $\langle F_{\mathrm{max}}\rangle$, of the varying lateral force. Using our model calculations to explore the relation between these two quantities (Fig. 1), we come to several unexpected and important conclusions. The solid curve in Fig. 1 was calculated by varying the potential corrugation U_0, for typical values of the system parameters. Different symbols in the figure represent calculations for a given U_0 but different combinations of the effective mass m and the temperature T. Interestingly, all data collapse on a single curve. The same is true for other scanning velocities (not shown here).

For the SS regime this "universal" character is easy to understand. In view of the sawtoothlike shape of the force-vs-position curve in this regime, one finds to a good approximation that $\langle F\rangle=(\langle F_{\mathrm{max}}\rangle+\langle F_{\mathrm{min}}\rangle)/2$. The difference between $\langle F_{\mathrm{max}}\rangle$ and $\langle F_{\mathrm{min}}\rangle$ is completely determined by the tooth slope, which depends on U_0, the effective spring constant, $k_{\mathrm{eff}}=(k^{-1}+K^{-1})^{-1}$, and the lattice constant a. This, in turn, completely fixes the $\langle F\rangle$-vs-$\langle F_{\mathrm{max}}\rangle$ relation. The values of the other parameters, m, T, and V, are required to fix the rates of thermally activated jumps and thus the $\langle F_{\mathrm{max}}\rangle$ value at which the slip events set in, on average. This determines with which point on the curve each specific parameter combination corresponds.

Outside the SS regime the curve is no longer truly universal. Rather than k_{eff}, the specific (k,K) combination becomes important, and for each cantilever (K) a separate universal curve is obtained, as is illustrated by the solid and dashed lines in Fig. 1. Importantly, the shapes of the curves are nontrivial and they allow one to distinguish between various

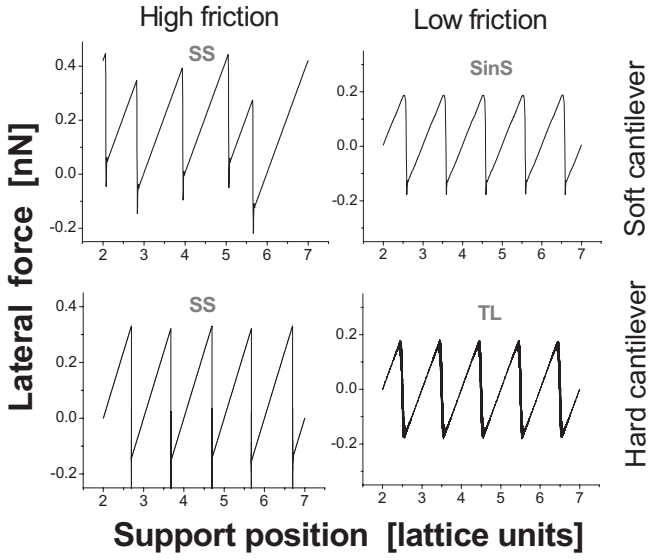

FIG. 2. Inherent dynamics of the two-mass-two-spring system (no thermal noise on the cantilever) in the SS and low-dissipation regimes (SinS and TL). Lateral force as a function of the support position (Vt), calculated for the cases of a soft and a hard driving spring (system parameters are specified in the captions of Figs. 3 and 4). The corrugation of the interaction potential was U_0=0.6 eV (top-left panel), 0.75 eV (bottom-left), 0.2 eV (top-right), and 0.25 eV (bottom-right).

low-dissipation sliding regimes, when the measuring system (M) experiences an effective potential (free energy[7]) averaged over rapid activated jumps of m. The response[9] depends on the relation between the corrugation of this effective potential and K. Sufficiently soft cantilevers, e.g., with $K \sim k$, exhibit regular stick-slip behavior (see top-right panel in Fig. 2), which is counterintuitive in view of the slipperiness of the contact. The friction in this SinS regime is low but finite (solid curve in Fig. 1). For hard cantilevers ($K \gg k$) the effective corrugation is not sufficient to produce mechanical instabilities. They will perform a nearly frictionless, continuous sliding (see bottom-right panel in Fig. 2), analogous to naive, mechanistic superlubricity but actually induced by thermal activation of the tip-apex motion. This is the regime of *true thermolubricity* (dashed curve in Fig. 1). Note that the one-spring model does not distinguish between these two physically different types of thermolubricity, SinS and TL but reveals some intermediate behavior, as shown schematically by the dotted curve in Fig. 1.

In view of its universal character and sensitivity to the friction regimes at play, the $\langle F \rangle$-vs-$\langle F_{\max} \rangle$ plot allows us to check the consistency between theory and experiment practically without using any adjustable parameter (see note[14]). Of course, some information is lost at this stage since this process does not yield the potential corrugations U_0 to which points on the plot correspond. For that, a more detailed analysis is required of the lateral force as a function of the support position or, simply, time. We will show that in this way U_0 can be found with relatively high precision, in spite of a big uncertainty in the value of the effective mass.

Of course, these ideas can be applied to FFM experiments provided the maximal values ($F_{\max}$) of the varying lateral force can be clearly identified. The force maxima can be distinguished easily in the stick-slip regime. On the other hand, one might expect a fluctuating, if not fully stochastic behavior of the force in the low-dissipation regimes. Actually, this is not the case. The inherent dynamics of the system both in the SinS and TL regimes turns out to be very regular, even more regular than in the SS regime, as can be seen in Fig. 2 (for more details see Ref. 9). This counterintuitive result reflects the nearly complete averaging of the effective tip-surface interaction, as experienced by the measuring system, over the rapid activated jumps of the tip's apex. Not more than a weak signature of incomplete averaging is sometimes observed in these regimes, in particular, in the right-bottom panel of Fig. 2. As shown earlier,[9] really stochastic behavior of the lateral force (*stochastic stick-slip*, SSS) takes place only in the case of a hard driving spring and only in a vary narrow range of the system parameters. Thus, a relatively sharp transition from SS to TL is found in the shape of the dashed curve in Fig. 1. This inherent dynamics of the system makes the force maxima extremely well defined. Below we show that it is nothing more than the trivial effect of thermal noise on the cantilever that makes the observable force loops look noisy. In the case of a hard cantilever this complication turns out to be not essential. For a soft cantilever irregularities become strong, indeed, but one can still distinguish force maxima appearing with the lattice periodicity. Consequently, the procedure of identifying $F_{\max}$ remains meaningful also in this case.

III. COMPARISON WITH EXPERIMENTS

Now we concentrate on two highly informative FFM experiments,[3,4] in which the transition from dissipative stick slip to nearly frictionless sliding has been reported. The potential corrugation has been varied in these experiments (though not controlled or measured directly), in one case by turning the tip with respect to the substrate[3] and in the other by changing the normal load.[4] Seemingly reasonable correspondence with the traditional one-spring model was observed in both cases and vanishing friction was attributed to the naively expected mechanistic superlubricity. Subsequent analysis[13] indicated that suppression of friction in the experiment of Ref. 3 took place already above the threshold of mechanistic superlubricity and hence had a thermal nature. However, the signature of a hidden discrepancy was present in the peculiar values of the pre-exponential factors of the jump rates extracted from both experiments.[13] Also unexplained was the very stochastic behavior of the lateral force recorded in one experiment,[3] in contrast to a very regular behavior in the other.[4] Our calculations provide a full and quantitative account of all these observations and, importantly, force us to revise the interpretation of the experiments.

In Figs. 3 and 4 we compare our calculations with experimental data from the papers mentioned above. The only essential difference between the parameters for the two experiments is a considerable difference in the stiffness K of the cantilevers used, one being extremely soft ($K \sim k$) and the other being hard ($K \gg k$). First of all one notices in both Figs.

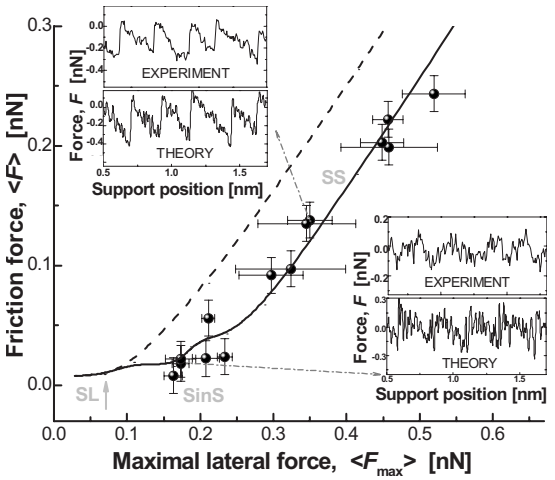

FIG. 3. Theory vs experiment: vanishing friction in a soft system. Experimental data were taken from Ref. 3. Parameters known from the experiment: cantilever stiffness $K=5.75$ N/m, tip-apex stiffness $k=2.6$ N/m, substrate lattice constant $a=0.246$ nm (graphite), cantilever+tip mass $M=1.2\times10^{-8}$ kg, temperature $T=300$ K, and scanning velocity $V=30$ nm/s. The effective tip-apex mass was set to $m=1\times10^{-20}$ kg (Ref. 7). The solid curve was calculated by varying the potential corrugation U_0. The dashed curve corresponds to the mechanistic Prandtl-Tomlinson model. Insets compare experimental and theoretical force-vs-position scans in the SS regime (top-left, $U_0=0.55$ eV) and at low force levels (bottom-right, $U_0=0.1$ eV). Note that in the experiment (Refs. 3 and 4) lateral forces opposite to the direction of motion were defined as negative (see insets), i.e., different from the definition used in our calculation; for the sake of comparison, we have adopted the same sign in the theory panels of the insets.

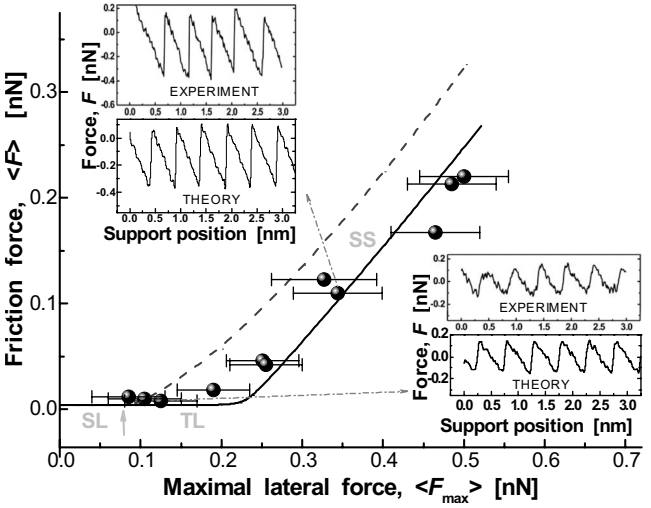

FIG. 4. Theory vs experiment: vanishing friction in a hard system. Experimental data were taken from Ref. 4. Parameters known from the experiment: $K=29$ N/m, $k=1.1$ N/m, $a=0.5$ nm (NaCl), $M=5.5\times10^{-11}$ kg, $T=300$ K, and $V=3$ nm/s. The rest is similar to Fig. 3. The corrugation of the interaction potential in the calculations shown in the insets was $U_0=0.8$ eV (top-left) and 0.2 eV (bottom-right).

3 and 4 the excellent agreement between the theoretical and experimental $\langle F\rangle$-vs-$\langle F_{\max}\rangle$ plots, which proves the consistency between our advanced model and both experiments. We emphasize that this comparison is practically free of adjustable parameters and that it is independent of the particular values of the potential corrugation behind each experimental point, which are not known yet at this stage. The plot is also not sensitive to the effective mass m of the tip apex, which is likely somewhat different for different experiments. Furthermore, in both cases considered, the positions of the experimental points with respect to the dashed lines (corresponding to the mechanistic Prandtl-Tomlinson model) unambiguously indicate that nearly vanishing friction was observed well above the threshold for true superlubricity. This provides us with a direct proof of the thermolubricity-induced ultralow-friction force of both Refs. 3 and 4. Moreover, the different shapes of the solid curves in Figs. 3 and 4 indicate the physically different low-dissipation regimes, namely, SinS in the "soft" system and TL in the "hard" one.

In addition to the shapes of the curves in Figs. 3 and 4 we can further verify the assignment of the dissipation regimes by a detailed inspection of individual traces of the lateral force as a function of the tip position. Characteristic examples are shown in the insets of Figs. 3 and 4. For the upper experimental points in both figures one observes ordinary stick-sliplike variations in the force, with the usual fluctuations of $F_{\max}$ while for the lower points the situation is different. In order to elucidate the inherent dynamics of the system at these lower forces we first consider the hypothetical case of zero thermal noise on the cantilever (see Fig. 2). For the soft system calculations at these low forces show absolutely regular stick-slip motion with highly symmetric positive and negative variations in the force ($F_{\min}$ is close to $-F_{\max}$) and a very small mean friction force as a result (top-right panel in Fig. 2). Meanwhile the tip apex is seen to be completely delocalized by rapid jumps between the substrate lattice positions. This is the manifestation of the *stuck-in-slipperiness* regime (for more details we refer to Ref. 9, where the full variety of possible regimes has been discussed). In contrast, the low-dissipation regime for the hard system (bottom-right panel in Fig. 2) is characterized by very regular and smooth sliding with nearly zero mean friction force, the manifestation of *true thermolubricity*.

When we include thermal noise in our calculations, we obtain force-vs-position graphs in nearly one-to-one correspondence with the experimental scans, both in the high- and low-dissipation regimes and both for the soft and hard systems (see insets of Figs. 3 and 4). This is in spite of the simplifications in the model of a 1D geometry and a sinusoidal potential. A remarkable "bonus" at this stage is that we can now estimate the true potential corrugation U_0 for each experimental scan with relatively high accuracy, at least in the SS regime, even though we have no more than a rough estimate for the effective mass m of the tip apex of 10^{-20} kg. The reason for this is that U_0 is a crucial parameter both for the mechanistic properties of the system and for the thermally activated motion, for which it works exponentially strong while m enters only the rate of activated jumps, as $m^{-1/2}$. As an example, let us assume an uncertainty in m as large as 4 orders of magnitude, $m=10^{20\pm2}$ kg. If we consider the fifth experimental data point from the top in Fig. 3, this introduces only a modest uncertainty in the potential,

$U_0 = 0.55 \pm 0.05$ eV. Note that the apparent U_0, as seen within the traditional model, would in this case be as low as 0.17 eV.

Finally, our calculations reproduce the very stochastic behavior of the lateral force in the low-dissipation regime of the soft system (bottom-right inset of Fig. 3) but very regular forces in the hard system (insets of Fig. 4). We have encountered a twofold manifestation of thermal noise; in the soft system the amplitudes of thermal fluctuations in the cantilever position are strong enough to cause sizable changes in the potential landscape seen by the tip apex and, hence, in the corresponding response of the recorded force while in the hard system this effect is small. As a consequence, the inherently regular motion in the SinS regime, characteristic for the soft system, is nearly completely ruined by fluctuations while in the hard system the inherently regular behavior characteristic for the TL regime remains.

IV. CONCLUSION

In summary, we have analyzed basic nanotribology experiments using an advanced two-mass-two-spring model that explicitly takes into account the ultralow effective mass of the tip apex. We have shown that by introducing the second spring the extended model not only leads to a more detailed description of atomic-scale friction (as shown in Ref. 8) but actually reveals a principal inconsistency of the traditional analysis of experimental results, involving a fatal underestimate of the corrugation of the interaction potential. We have introduced a consistent, fully quantitative approach, based on a universal relation between basic observables. Combining this analysis, free of adjustable parameters, with detailed calculations of the lateral force dynamics we find excellent agreement with the observations of nearly vanishing friction of Refs. 3 and 4. In contrast with their original interpretation, we conclude that friction has not been ultralow in these experiments due to straightforward mechanistic superlubricity but rather due to a specific, thermally induced form of stick-slip motion (SinS) in the first case and due to genuine thermolubricity in the second. As far as the FFM tip is a good model for the asperities that constitute the contact between macroscopic sliding bodies, a more general speculation can be made. Thermally assisted dynamics is much more dominant in friction than one thought, which might provide interesting opportunities for low-friction applications.

*Permanent address: Institute of Physical Chemistry and Electrochemistry, Russian Academy of Sciences, Leninsky Prospect 31, 119991 Moscow, Russia; krylov@physics.leidenuniv.nl

[1] C. M. Mate, G. M. McClelland, R. Erlandsson, and S. Chiang, Phys. Rev. Lett. **59**, 1942 (1987).
[2] R. W. Carpick and M. Salmeron, Chem. Rev. (Washington, D.C.) **97**, 1163 (1997).
[3] M. Dienwiebel, G. S. Verhoeven, N. Pradeep, J. W. M. Frenken, J. A. Heimberg, and H. W. Zandbergen, Phys. Rev. Lett. **92**, 126101 (2004).
[4] A. Socoliuc, R. Bennewitz, E. Gnecco, and E. Meyer, Phys. Rev. Lett. **92**, 134301 (2004).
[5] M. H. Müser, M. Urbakh, and M. O. Robbins, Adv. Chem. Phys. **126**, 187 (2003).
[6] S. Maier, Y. Sang, T. Filleter, M. Grant, R. Bennewitz, E. Gnecco, and E. Meyer, Phys. Rev. B **72**, 245418 (2005).
[7] S. Yu. Krylov, J. A. Dijksman, W. A. van Loo, and J. W. M. Frenken, Phys. Rev. Lett. **97**, 166103 (2006).
[8] D. G. Abel, S. Y. Krylov, and J. W. M. Frenken, Phys. Rev. Lett. **99**, 166102 (2007).
[9] S. Yu. Krylov and J. W. M. Frenken, New J. Phys. **9**, 398 (2007).
[10] S. Yu. Krylov and J. W. M. Frenken, J. Phys.: Condens. Matter **20**, 354003 (2008).
[11] E. Gnecco, R. Bennewitz, T. Gyalog, C. Loppacher, M. Bammerlin, E. Meyer, and H.-J. Güntherodt, Phys. Rev. Lett. **84**, 1172 (2000).
[12] Z. Tshiprut, S. Zelner, and M. Urbakh, Phys. Rev. Lett. **102**, 136102 (2009).
[13] S. Yu. Krylov, K. B. Jinesh, H. Valk, M. Dienwiebel, and J. W. M. Frenken, Phys. Rev. E **71**, 065101(R) (2005).
[14] To be precise, there is an important system parameter, the effective stiffness of the tip apex k, that influences the shape of the universal curve. Its value can be found directly and with relatively high precision from measurements of the force-vs-position slope at stick events in SS regime.